Marine Geology 395 (2018) 14–21

Contents lists available at ScienceDirect

Marine Geology

journal homepage: www.elsevier.com/locate/margo

Impact of seasonal vertical stratification on the dispersion patterns of dredging plumes off the south coast of Korea

Jun Young Seo[a], Ho Kyung Ha[a,*], Jungho Im[b], Jin Hwan Hwang[c], Sun Min Choi[a], Nam-Il Won[d], Youngsung Kim[d]

[a] Department of Ocean Sciences, Inha University, Incheon 22212, South Korea
[b] School of Urban and Environmental Engineering, Ulsan National Institute of Science and Technology, Ulsan 44919, South Korea
[c] Department of Civil and Environmental Engineering, Seoul National University, Seoul 08826, South Korea
[d] Korea Water Resources Corporation, Daejeon 34350, South Korea

ARTICLE INFO

Keywords:
Sand dredging
Plumes
Overflow
Stratification
Dispersion patterns

ABSTRACT

Simultaneous satellite and ship-borne surveys have been conducted to investigate the dispersion patterns of dredging plumes off the south coast of Korea in two contrasting seasons (spring and autumn). The distribution of total suspended solid (TSS) derived from sequential satellite imagery showed that the dredging plumes in spring developed over longer distances along the surface current than those in autumn. In spring, the deep and strong stratified condition in the water column contributed to the increase in radius of plume dispersion along the water surface. In autumn, the shallow and vertically well-mixed (or un-stratified) condition in the water column enhanced sinking of suspended dredged materials. This difference is due to the Brunt-Väisälä frequency being higher in spring ($0.0183\ s^{-1}$) than in autumn ($0.0123\ s^{-1}$). Although the sediment-laden overflow significantly increased TSS near the surface during the dredging period, the TSS contribution to water column stratification was only 2.3 − 5.6% of the thermohaline contribution. Therefore, the seasonal variation of thermohaline density is the main factor determining the dispersion patterns of dredging plumes in the study area.

1. Introduction

Over the past few decades, sands have been increasingly dredged to meet the demands for sand resources used for beach nourishment and land reclamation (Suedel et al., 2008). In the dredging operation, overflows with high-concentration suspended sediment produce turbid plumes at the water surface; these can be dispersed over several tens of kilometers under combined conditions of oceanic (e.g., current and tide) and atmospheric (e.g., wind) forcings (Pennekamp et al., 1996; Teeter, 2000). Such anthropogenic activities generate serious disturbances to aquatic ecosystems with adverse environmental impacts (Shao et al., 2015). Due to the increased turbidity, for instance, sunlight can be temporarily blocked, thus decreasing primary production significantly near the water surface (Rogers, 1990; Erftemeijer and Lewis, 2006; Suedel et al., 2008). Also, the dredging process itself often dislodges toxic pollutants residing in benthic layers, and releases them into the overlying water column, leading to the degradation of water quality (Messieh et al., 1991; Gilkinson et al., 2003; Du Four and Van Lancker, 2008; Padmalal et al., 2008). Although dredging is necessary in practice to meet growing commercial demands, field-based, synoptic observations are required to understand the environmental issues associated with the aforementioned problems (Nichols et al., 1990; Hitchcock and Bell, 2004; Roman-Sierra et al., 2011).

Different types of dredgers are available for excavating bottom sediments. For instance, hydraulic type dredgers transport bottom sediments in the form of a "sediment-water mixture," which is pumped through a pipeline to a barge used for storing the dredged sands (Manap and Voulvoulis, 2015). Coarse-grained sediments are retained on the barge, but the fine-grained fraction and excess water overflow into the surrounding water. The overflow released from the barge has been investigated to understand the main mechanisms for dispersion in previous studies (Pennekamp et al., 1996; Fettweis et al., 2011; Cutroneo et al., 2012; Manap and Voulvoulis, 2015). Nonetheless, little is known about the seasonal variations of dispersion process of suspended sediments within the dredging plume. In this aspect, the dredging in south coast of Korea gave an opportunity to understand the relationship between dredging plume dispersion and seasonal variation of water column structure.

In this study, therefore, several field surveys were performed to investigate the seasonal dispersion patterns of offshore sand dredging

* Corresponding author.
E-mail address: hahk@inha.ac.kr (H.K. Ha).

http://dx.doi.org/10.1016/j.margeo.2017.09.005
Received 19 December 2016; Received in revised form 7 September 2017; Accepted 10 September 2017
Available online 14 September 2017
0025-3227/

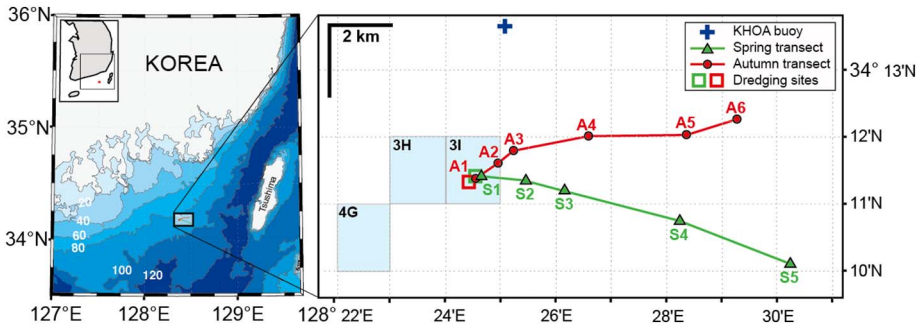

Fig. 1. Map showing bathymetry (20-m interval), dredging sites, ship-borne survey stations, and location of current-measuring KHOA buoy. Triangles (green) and dots (red) indicate hydrocast stations along the transects. Light blue areas labeled 3H, 3I, and 4G represent the dredging complexes (mean depth: 84 m). (For interpretation of the references to color in this figure legend, the reader is referred to the web version of this article.)

plumes. Simultaneous satellite and ship-borne data were collected to reveal the spatial and temporal variations of plumes in two contrasting seasons (spring and autumn). The main objectives were (1) to estimate the radius of plume dispersion resulting from seasonality in the water column structure, and (2) to reveal the main factor determining the dispersion patterns.

2. Study area

The study area located on the continental shelf off the south coast of the Korean Peninsula exhibits complex hydrodynamic conditions (Fig. 1). This area has a typical semi-diurnal, micro-tidal (< 2 m) regime. The tidal current flows SW-ward during flood and NE-ward during ebb (Kim et al., 2011). The typical wave propagates S- or SW-ward, and mean significant wave height is about 0.5 to 1.5 m (You and Park, 2010).

The intrusions of Tsushima Warm Current (TWC) and South Korean Coastal Water (SKCW) and wind patterns of the Asian monsoon are main factors influencing on the variation of water column structure (Oscar, 1982). In spring, the temperature and salinity are still cold and saline despite increase in the intrusion of NE-ward TWC, resulting in development of deep and stratified layer. In autumn, meanwhile, the expansion of SKCW by northwesterly wind (mean speed: 8.3–8.8 m s^{-1}) begins breakup of the pycnocline, causing the deepening of mixed layer down to 40 m depth (Oscar, 1982; Lee et al., 2007; Kim H.G. et al., 2014; Lee and Choi, 2015).

The slope of this area has a gradual seaward descent, and the depth is in the range of 72 to 95 m. The bottom is mainly composed of sands (3H: ca. 97.05%, 3I: ca. 93.36%, and 4G: ca. 88.85%), and the grain size distribution generally exhibits a coarsening-seaward trend (Cho et al., 1999; Chough et al., 2000; Lee et al., 2008; Jung et al., 2012; K-Water, 2013). In 2015, within three dredging complexes (3H, 3I, and 4G in Fig. 1), plain suction dredgers, of a typical hydraulic type, pumped sand loads of about 2000 to 5000 m^3 day^{-1} (Fig. 2). The sand loads were about 4870 and 3216 m^3 day^{-1} during the selected target dates (spring: May 19; autumn: October 18), respectively.

3. Materials and methods

The Geostationary Ocean Color Imager (GOCI) was used to evaluate the horizontal dispersion of the surface plumes in spring (March, April, and May) and autumn (September, October, and November). The satellite images were acquired from the Korea Ocean Satellite Center (http://kosc.kiost.ac.kr). GOCI is suitable for tracking the surface plumes with a high-temporal resolution (He et al., 2013; Lyu et al., 2015). It provides eight images per day from KST 9:30 AM to 16:30 PM with 1-hour interval at six visible (412, 443, 490, 555, 660, and 680 nm) and two near-infrared (745 and 865 nm) bands with 500 × 500 m pixel size (Choi et al., 2012; Kim Y.H. et al., 2014; Ke et al., 2015). Since GOCI has an optical sensor, its data collection is very sensitive to weather conditions such as cloud cover (Jang et al., 2017). In the image processing, pixels covered by clouds were discarded. GOCI provides a Level 1B (L1B) product, which was corrected through the image pre-processing system by radiometric and geometric corrections (Ryu et al., 2012). The L1B product was converted through the GOCI data processing system with Yellow and East China Sea Ocean Color (YOC) algorithms to Level 2A products including three basic outputs—chlorophyll-*a* concentration, total suspended solid (TSS in mg l^{-1}), and colored dissolved organic matter (Tassan, 1994; Ruddick et al., 2012; Son et al., 2014). In particular, the output of band 4 (green band) was used to retrieve the TSS. The plume dispersion velocities were calculated from the positional shifts of TSS in sequential GOCI imagery with 1-hour interval.

A series of ship-borne surveys had been conducted along the major axis of plume to measure water column vertical profiles at the same times as those of the GOCI image collection. In both spring and autumn, the ship-borne surveys were conducted during ebb-to-flood and flood-to-ebb phases in spring tide, respectively. Among the ship-borne surveys, representative data collected in spring (May 19, 2015) and autumn (October 18, 2015) were selectively analyzed in this study to compare the characteristic seasonality in the dispersion patterns. In both seasons, profiles of temperature, salinity and turbidity were acquired by taking hydrocasts with a conductivity-temperature-depth sensor (CTD; SBE 19plus, Sea-Bird Electronics) with an attached optical backscatter sensor (OBS; OBS-3+, Campbell Scientific). During the upcasts, 10 water samples were collected using a pump at selected levels (1, 3, 6, 9, 15, 20, 25, 30, 35, and 40 m) to calibrate the backscatter signal (in nephelometric turbidity unit, NTU) from the OBS. In total, 135 water samples were filtered by vacuum filtration on pre-weighed glass fiber filters (GF/F; pore size: 0.7 μm). The filters were oven-dried at 105 °C for 24 h. The actual TSS was determined from the weight difference of reweighed filters. The data exhibited a good linear regression (r^2 = 0.85, see Online Supplementary Figure) between backscatter signal and filtered TSS.

The surface current data were downloaded from an ocean buoy operated by the Korea Hydrographic and Oceanographic Agency (KHOA; http://www.khoa.go.kr). Buoy location (34°13′21″N, 128°25′08″E) was about 4.3 km away from the dredging sites (Fig. 1). The current was recorded at 3 m depth by a Doppler Current Sensor (DCS 4420, Aanderaa Data Instruments) every 30 min.

4. Results

The turbid plumes produced by dredging exhibited different dispersion patterns in the two contrasting seasons (spring and autumn). The surface distribution of TSS derived from sequential satellite imagery showed that the dredging plumes in spring developed over longer distances along the water surface than those in autumn (Fig. 3). Plume radius changed significantly with month. In March, the plumes were not actively dispersed, being confined within a radius of about 10 km from the dredging complex, even though the dredging was being continuously conducted (Fig. 3a and b). In April and May, they were dispersed E- or SE-ward along the water surface (Fig. 3c, d, e, and f). Notably, the extensive dispersion of plumes in May indicates that they